



HAL
open science

Pulmonary delivery of pyrazinamide-loaded large porous particles

Dinh-Duy Pham, Nicolas Grégoire, William Couet, Claire Gueutin, Elias Fattal, Nicolas Tsapis

► **To cite this version:**

Dinh-Duy Pham, Nicolas Grégoire, William Couet, Claire Gueutin, Elias Fattal, et al.. Pulmonary delivery of pyrazinamide-loaded large porous particles. *European Journal of Pharmaceutics and Biopharmaceutics*, 2015, 94, pp.241-250. 10.1016/j.ejpb.2015.05.021 . hal-02478095

HAL Id: hal-02478095

<https://hal.science/hal-02478095>

Submitted on 28 Jul 2023

HAL is a multi-disciplinary open access archive for the deposit and dissemination of scientific research documents, whether they are published or not. The documents may come from teaching and research institutions in France or abroad, or from public or private research centers.

L'archive ouverte pluridisciplinaire **HAL**, est destinée au dépôt et à la diffusion de documents scientifiques de niveau recherche, publiés ou non, émanant des établissements d'enseignement et de recherche français ou étrangers, des laboratoires publics ou privés.

Pulmonary delivery of pyrazinamide-loaded large porous particles

Dinh-Duy Pham^{1,2,3,4}, Nicolas Grégoire⁵, William Couet⁵, Claire Gueutin¹, Elias Fattal¹, Nicolas Tsapis¹

1. Univ Paris-Sud, Institut Galien Paris-Sud, CNRS UMR 8612, LabEx LERMIT, Châtenay-Malabry, France.
2. University of Medicine and Pharmacy, Faculty of Pharmacy, Pharmaceutics Department, Ho Chi Minh City, Vietnam
3. Division of Pharmacotechnology and Biopharmacy, Ton Duc Thang University, Ho Chi Minh City, Vietnam.
4. Faculty of Applied Sciences, Ton Duc Thang University, Ho Chi Minh City, Vietnam.
5. Univ Poitiers, INSERM U1070, France

Corresponding authors :

- N. Tsapis Univ Paris Sud, UMR CNRS 8612, Faculté de Pharmacie, 5 Rue Jean-Baptiste Clément, 92296 Châtenay-Malabry, France. nicolas.tsapis@u-psud.fr
- D. D Pham University of Medicine and Pharmacy, Faculty of Pharmacy, 41-43 Dinh Tien Hoang, District 1, Ho Chi Minh City, VietNam. duyphamdinh1981@gmail.com
- D. D. Pham, Ton Duc Thang University, Faculty of Applied Science, Division of Pharmacotechnology and Biopharmacy, No. 19 Nguyen Huu Tho Street, Tan Phong Ward, District 7, Ho Chi Minh City, VietNam. phamdinhduy@tdt.edu.vn

Abstract

We have improved the aerodynamic properties of pyrazinamide loaded large porous particles (PZA-LPPs) designed for pulmonary delivery. To overcome the segregation of the different components occurring during the spray drying process and to obtain homogeneous LPPs, spray drying parameters were modified to decrease the drying speed. As a result, good aerodynamic properties for lung delivery were obtained with a fine particle fraction (FPF) of 40.1 ± 1.0 % and an alveolar fraction (AF) of 29.6 ± 3.1 %, a mass median aerodynamic diameter ($MMAD_{aer}$) of 4.1 ± 0.2 μm and a geometric standard deviation (GSD) of 2.16 ± 0.16 . Plasma and epithelial lining fluid (ELF) concentrations of pyrazinamide were evaluated after intratracheal insufflation of PZA-LPPs ($4.22 \text{ mg}\cdot\text{kg}^{-1}$) into rats and compared to intravenous administration (iv) of a pyrazinamide solution ($5.82 \text{ mg}\cdot\text{kg}^{-1}$). The *in vivo* pharmacokinetic evaluation of PZA-LPPs in rats reveals that intratracheal insufflation of PZA-LPPs leads to a rapid absorption in plasma with an absolute bioavailability of 66%. This proves that PZA-LPPs dissolve fast upon deposition and that PZA crosses efficiently the lung barrier to reach the systemic circulation. PZA concentrations were 1.28-fold higher in ELF after intratracheal administration than after *iv* administration and the ratio of ELF concentrations over plasma concentrations was 2-fold greater. Although these improvements are moderate, lung delivery of PZA appears an interesting alternative to oral delivery of the molecule and should now be tested in an infected animal model to evaluate its efficacy against *Mycobacterium tuberculosis*.

Keywords: Tuberculosis, Pyrazinamide, Lung delivery, Aerodynamic properties, Pharmacokinetics.

1. Introduction

Tuberculosis (TB) is an infectious disease due to *Mycobacterium tuberculosis*, affecting mainly the lungs [1]. TB current treatment, as recommended by the WHO, consists of a combination of orally-administered four first-line drugs: isoniazid, rifampicin, ethambutol and pyrazinamide [2-4]. Despite the efficacy of the TB regimen, the emergence of drug-resistant strains of *M. tuberculosis* and the lack of new anti-TB drugs represent a threat for the containment of TB epidemic. Two problems are responsible for the emergence of drug-resistance: some patients do not comply with the long treatments required and mycobacteria may be exposed to sub-therapeutic levels of antibiotics [5, 6]. In patients, numerous bacteria populate lung lesions leading to the formation of granulomas. Due to the characteristics of these granulomas, conventional oral and parenteral therapies are inefficient in providing therapeutic levels of anti-TB drugs to bacteria sequestered therein. Among therapeutic molecules, pyrazinamide (PZA) is particularly interesting as it is active against a population of non-growing, persistent tubercle bacilli that other TB drugs cannot destroy [7-9]. These bacilli are present in the above-described lung lesions. The fraction of PZA reaching these lesions after oral administration therefore helps to shorten TB treatment. Pulmonary delivery of anti-tubercular drugs has been proposed as an alternative strategy to obtain higher drug concentrations close to the granulomatous lesions [10, 11]. Since the lungs are directly targeted, total body doses are lower, leading to a decrease of potential drug resistance build-up. This is of particular interest for PZA to favor high drug concentration in the vicinity of sequestered bacteria and facilitate their eradication.

Anti-TB drugs can be delivered to the lungs by nebulization [12] [13, 14] or as dry powders for inhalation [15-18]. Among dry powders for inhalation, large porous particles (LPPs) have

emerged since the end of the 90's for both local and systemic treatments due to their efficient deposition in the lungs using simple inhalation devices [19-22]. By taking advantage of the LPP technology, TB treatment could be more efficient since antibiotics would be delivered directly to the site of infection to yield therapeutic local drug concentrations with lower systemic exposure than oral delivery [10].

PZA-LPPs were previously optimized by spray drying using excipients preventing PZA recrystallization and promoting particle stability [23]. Herein, we present the *in vitro* characterization of the aerodynamic properties of PZA-LPPs. PZA-LPPs were also administered to rats by insufflations and a thorough evaluation of the drug pharmacokinetics and broncho-alveolar lavage content was performed and compared with an iv administration of PZA through a pharmacokinetic model.

2. Materials and Methods

2.1. Materials

Pyrazinamide (PZA) was obtained from Fluka, with specified purity greater than 99%. 1,2-dipalmitoyl-sn-glycero-3-phosphatidylcholine (DPPC) was provided by Corden Pharma (Switzerland) and hyaluronic acid, sodium salt 95% (MW=1000 kDa) by Acros organics. Ammonium bicarbonate, acetazolamide and DL-Leucin were provided by Sigma–Aldrich (France). Ethanol absolute in analytical grade was obtained from Carlo Erba Reagents (France). Water was purified using a RIOS/MilliQ system from Millipore (France). HPLC-grade acetonitrile and methanol were purchased from Prolabo (France).

2.2. Particle formulation via spray drying

Large porous particles were obtained by spray drying using a mini spray dryer Büchi B-290 (Flawil, Switzerland) equipped with a 0.7 mm diameter two-fluid nozzle, which operates in a co-current mode. The formulation chosen was previously optimized in terms of composition [23] to prevent PZA recrystallization and yield stable large porous particles. The spray drying parameters such as air-flow rate, feed-flow rate, inlet temperature and aspiration are reported in Table 1. Briefly, DPPC was dissolved into 700 mL ethanol, whereas PZA and Leu were dissolved into 300 mL water. Then, hyaluronic acid was added into the aqueous solution and stirred using a magnetic stir bar for about a hour until dissolution. Afterwards, ammonium bicarbonate was dissolved into the aqueous solution and subsequently ethanolic and aqueous solutions were mixed immediately prior to atomization. The final concentration of ammonium bicarbonate in the ethanol/water mixture was 2 g/L. The final solid content of the solution was 2 g/L omitting ammonium bicarbonate since this compound decomposes into water and gas during the drying process. Powder samples were stored at room temperature under vacuum in a desiccator immediately after spray drying to limit moisture uptake by samples between production and testing. The yield was calculated as a percentage by dividing the mass of the powder collected by the initial mass of solids in the solution prior to spray drying.

Characterization of spray-dried powders

Particle size distribution was measured by light diffraction using a Mastersizer 2000 equipped with a Scirocco dry disperser (Malvern Instruments, France) at a dispersing pressure of 1 bar. The refractive index used was 1.5. Values presented are the average of at least 3

determinations, errors bars indicate the standard deviation (S.D.). The powder density was evaluated by tap density measurements using a tapping apparatus (Pharma test PT-TD1). Tap density (ρ) was measured in a 10 mL glass graduated cylinder filled with a fixed initial volume of powder around 8 mL. The tap density was determined after 1000 taps from a constant height. Measurements were performed in duplicate. The morphology of particles was examined by scanning electron microscopy (SEM) using a LEO1530 microscope (LEO Electron Microscopy Inc., Thorn-wood, NY) and operating between 1 and 3 kV with a filament current of about 0.5 mA. Powder samples were deposited on a carbon conductive double-sided tape (Euromedex, France). They were coated with a palladium–platinum layer of about 4 nm, using a Cressington sputter-coater 208HR with a rotary planetary-tilt stage, equipped with a MTM-20 thickness controller. The thermal properties of the powders were analyzed using differential scanning calorimetry (DSC) (DSC7, PerkinElmer, USA). Thermograms were analyzed using *Pyris* software. An empty aluminum pan was used as the reference for all measurements. A sample (1-5 mg) of powder was placed in hermetically sealed 40 μ l aluminum pan and analyzed. DSC runs were conducted from 30 to 210 °C at a rate of 10 °C/min. Calibration was achieved using Indium ($T_{\text{onset}} = 156.60$ °C) as well as Zinc ($T_{\text{onset}} = 419.47$ °C). The onset and peak temperatures and enthalpy of transition (ΔH) were determined for each peak. Powder crystallinity was analyzed using X-ray powder diffraction (XRPD). XRPD patterns were measured on a Bruker D2 diffractometer equipped with a XFlash detector in SPMS laboratory – Centre of diffraction – École Centrale Paris using Ni-filtered $\text{CuK}\alpha$ radiation. Data were collected over an angular range comprised between 5 and 40° (2θ) with a step size of 0.01°, a counting time of 5 s/step.

2.3. Powder stability

Powder stability was assessed by leaving samples to age at room temperature under vacuum in a desiccator (temperature comprised between 15 and 25 °C). Particle size was performed on aged samples at $t = 0, 2$ and 4 weeks.

2.4. Drug Content

The content of PZA in the powder was determined by UV-Visible double beam spectrophotometer (Lambda 25, PerkinElmer, France) with 1 cm matched quartz cuvettes. 20 mg powder was accurately weighed and transferred into 20 mL volumetric flask. It was dissolved properly and diluted up to the mark with ethanol/water (70/30). Then, the solution was diluted to obtain a 10 $\mu\text{g/mL}$ solution. The absorbance of the solutions containing PZA was determined in the UV range 200-400 nm using an ethanol/water (70/30) blank. The standard curve was constructed by plotting the absorbance of pyrazinamide from 2 to 16 $\mu\text{g/mL}$ of PZA.

2.5. *In-vitro* aerodynamic evaluation

The aerodynamic properties of dry powders for inhalation were determined using multi-stage liquid impinger (MSLI, Apparatus C, European Pharmacopoeia 2008, Copley Scientific, Switzerland) through a dry-powder, breath-activated inhaler device (Aerolizer®, Novartis). Prior to testing, 20 mL of the solvent (ethanol/water, 70/30, v/v) was added into each of the four stages of the impinger. 5 mg dry powder was weighed and loaded into a size 4 hydroxypropylmethylcellulose capsules (LGA, France), further placed in the inhaler device. The inhaler device containing a filled capsule was fitted in the induction port. The capsule was then

punctured and the powder was delivered at a flow rate of 60 L/min for 4 s to simulate an inspiration. This process was repeated twice. The amount of powder deposited on the impinger stages, as well as the amount retained by the filter was assayed spectrophotometrically as described below. The solvent of each stage was collected, the filter was rinsed with ethanol/water (70/30, v/v) and the respective volumes were transferred into 50 mL volumetric flasks. Then, the volume was completed with ethanol/water, 70/30 (v/v). Aerodynamic evaluation was performed with normal powder and also a powder fluorescently labeled using 1% of Liss-Rhod-PE before spray-drying (Avanti Polar Lipids, USA). Calibration curves were prepared in the range of 5 – 100 $\mu\text{g}\cdot\text{mL}^{-1}$ powder by adding aliquots of the stock solutions of each sample in the 20 mL volumetric flasks. The stock solutions were prepared by dissolving 20 mg of the powder in 20 mL of ethanol/water, 70/30 (v/v). The volume was completed to 20 mL with ethanol/water, 70/30 (v/v). The absorbance values were measured at 268 nm (measuring PZA for normal powder) and at 564 nm (measuring LissRhod-PE for labeled powder) using a LS50B spectrofluorimeter (Perkin Elmer). The emitted fraction (EF) defined as the percent of total loaded powder mass exiting the capsule was determined gravimetrically and calculated using the following equation:

$$\text{EF} = \left(\frac{m_{\text{full}} - m_{\text{empty}}}{m_{\text{powder}}} \right) \times 100$$

Where m_{full} and m_{empty} are the masses of the capsule before and after simulating the inhalation and m_{powder} the mass of the powder placed in the capsule.

The cumulative mass of powder smaller than the stated size of each stage of the impinger was calculated and plotted on a log probability scale, as percent of total mass recovered in the impinger against the effective cut-off diameter. The cut-off diameter of each individual stage

were 13.0, 6.8, 3.1 and 1.7 μm for stages 1 to 4, respectively [24]. The experimental mass median aerodynamic diameter (MMAD_{aer}) of the particles was defined from this graph as the particle size at which the line crosses the 50% mark. And the geometric standard deviation (GSD) as $GSD = \sqrt{(\text{sizeX}/\text{sizeY})}$ where sizeX is the particle size for which the line crosses the 84% mark and sizeY the 16% mark. The fine particle fraction (FPF) was calculated by interpolation from the same plot as the fraction of powder emitted from the inhaler with an aerodynamic diameter $\leq 5 \mu\text{m}$ [24]. The alveolar fraction (AF) was calculated by interpolation from the same plot as the fraction of powder emitted from the inhaler with an aerodynamic diameter $\leq 3.1 \mu\text{m}$.

2.6. In-vivo studies

Animal model

Experiments have been conducted according to the European rules (86/609/EEC and 2010/63/EU) and the Principles of Laboratory Animal Care and legislation in force in France (Decree No. 2013-118 of February 1, 2013) under protocol 01800.01. Male Sprague Dawley rats were obtained from Harlan Laboratory (GANNAT, France). The animals weighed between 250 and 300 g. The animals were in good health upon arrival and remained so until use; no clinical signs of illness were observed at any time. They were housed 4 per cage while on study in accordance to EEC guidelines. The light/dark cycle was 12 h/12 h. The temperature in the animal room was ambient room temperature of approximately 25 °C and the ambient humidity was in the range of approximately 35–60%. Animals were allowed access to food and water ad libitum throughout the duration of the study.

Drug administration and sample collection

40 rats were divided into the following 2 groups (20 rats per group): Animals were anaesthetized with an intraperitoneal injection of ketamine (100 mg.kg^{-1}) and xylazine (10 mg.kg^{-1}) and then received a PZA dose by intratracheal insufflation of LPP-PZA powder, corresponding theoretically to 6 mg.kg^{-1} PZA or intravenous injection (iv) of $200 \mu\text{L}$ solution leading to a 5.82 mg.kg^{-1} PZA dose (glucose 5% to adjust osmolarity). For intratracheal insufflation, LPP-PZA powders were weighed out into capsules and stored in desiccators prior to dosing. The LPP-PZA powder was introduced into the lung through the DP-4 dry powder insufflator device (PennCentury, Philadelphia, PA). Once sedation was confirmed, animals were placed onto a modified slant board to optimize visual placement of the insufflation cannula into the trachea. The tip of the insufflation device was placed in the trachea just above the carina and 5 mg of LPP-PZA powder was delivered through the insufflation device by rapidly pushing a 2 cm^3 bolus of air through the device. The insufflator was weighed before and after powder filling as well as after administration to determine the actual dose insufflated per rat. For intravenous injection, the isotonic solution of PZA was injected into the jugular vein.

For each rat, blood was taken only at 3 different time points via the jugular vein. For each time point, bloods were taken from a minimum of 6 rats. Blood was collected at before PZA administration and $1/4$, $1/2$, 1, 2, 3, 4, 6, 18 and 24 hours following PZA administration (intratracheal or iv). Before taking the blood, the rats were anesthetized by isoflurane inhalation. Approximately 1 ml of blood was taken at each time point. All blood samples were collected in heparinized tubes. Plasma was separated in a tabletop centrifuge (Eppendorf

Minispin[®]) at 10,000 rpm for 10 min. The retrieved plasma was subsequently snap frozen on dry ice and stored at -80 °C until analysis by HPLC. Bronchoalveolar lavage fluids (BALFs) were collected to assess lung epithelial lining fluid (ELF) PZA levels after animals were deeply anaesthetized by isoflurane inhalation, euthanized by cutting the diaphragm, and exsanguinated by cardiac puncture. The trachea was cannulated using an 18 gauge needle adaptor for subsequent injection and retrieval of BALF. Briefly, aliquots of 8 mL of chilled PBS were instilled into lungs after intubating the trachea with a syringe fitted with tracheal cannula, an 18 gauge needle adaptor. The lungs were massaged and the fluid withdrawn immediately and collected in centrifuge tube kept on ice. This process was repeated 3 times for obtaining the most macrophage cells [25]. All lavages were pooled and centrifuged (1500 rpm; 10 min; 4 °C). The supernatant of lavage and the alveolar cell pellet were collected separately, snap-frozen on dry ice, and stored at -80 °C until analysis.

HPLC determination of PZA

Plasma, BALF and alveolar cell pellet PZA concentrations were determined by an HPLC assay described in the literature [26] with minor modifications. Briefly, all samples were analyzed using high-performance liquid chromatography (HPLC) with the following equipment: a Waters model 1525 binary pump and model in-line degasser AF, a model 717 plus autosampler, a model 2487 dual λ absorbance detector, a Dell computer and the Breeze version 3.30 SPA HPLC data management system. Chromatography was performed with a stainless steel Interchrom Spherisorb 5 μ m ODS2 column (250 mm x 4.6 mm, 5 μ m particle size). The mobile phase was 0.02M potassium phosphate buffer – acetonitrile mixture at pH 2.6, with a final acetonitrile

concentration of 2%. The flow-rate was set to 1 mL/min. The effluent was monitored at 268 nm with a detection scale of 0.1 or higher as needed. All measurements were performed at room temperature. The retention times for pyrazinamide and acetazolamide were 10.5 and 21.0 min, respectively. While BALF supernatants and AC samples were run for 36 min, plasma was run for 45 min because of late peaks that interfered with the next injection. The limit of quantification of PZA was found equal to 0.007 $\mu\text{g}/\text{mL}$.

Preparation of plasma standards and samples:

200 μL of spiked plasma (PZA concentrations from 0.5 to 80 $\mu\text{g}/\text{mL}$) or sample were deproteinated by adding 400 μl internal standard solution (10 mg/mL acetazolamide in acetonitrile), vortexing for 30 s, centrifuging at $3000 \times g$ for 10 min (7000 rpm for 10 min eppendorf), decanting into a clean glass tube, and evaporating to dryness under nitrogen. After the addition of 200 μL of mobile phase and vortexing, 50 μL were injected onto the column. The standard curve was constructed by plotting the peak-area ratios of pyrazinamide to acetazolamide against the spiked concentration of pyrazinamide (weighted as $1/y$ where y equals the concentration of pyrazinamide).

Preparation of BALF and Alveolar cell pellet standards and samples:

PBS was chosen as the matrix for standard curves and controls to measure pyrazinamide concentrations in both BALF and AC suspensions. It was ascertained that the slopes, y-intercepts, and linearity of these matrices were similar. Bronchial lavage fluid (around 24 mL) was centrifuged at $400 \times g$ for 10 min, and the cells separated from the supernatant

immediately after collection. The cells were resuspended in PBS to yield a tenfold (2 mL PBS) concentration of the original lavage fluid centrifuged. To lyse the cells, the suspension was sonicated at 40% amplitude for 2 min. The drug was extracted as follows: 0.5 mL of spiked PBS (PZA concentrations from 0.005 to 0.500 $\mu\text{g}/\text{mL}$), or 0.5 mL of diluted BAL supernatant were pipetted into screw cap glass tubes. Twenty microliters of internal standard solution (10 mg/mL acetazolamide in acetonitrile) and 50 μL of 35% hydrochloric acid were then added. After vortexing for 2 min, 4.0 mL of ethyl acetate was added, vortexed for 2 min, and then centrifuged for 10 min at $1000 \times g$. The organic phase was transferred to a clean tube, and the aqueous phase left in the screwcap tube was extracted again in the same manner. The resulting 8 mL of solvent was pooled, evaporated to dryness under nitrogen, and then reconstituted in 0.2 mL of mobile phase. Fifty microliters were injected into the column. The standard curve was constructed by plotting the peak-area ratios of pyrazinamide to acetazolamide against the spiked concentration of pyrazinamide (weighted as $1/y$ where y equals the concentration of pyrazinamide). PZA concentration in ELF was estimated from PZA BALF concentrations using a constant dilution factor for the lavage (2910)

Pharmacokinetic analysis

Concentrations versus time data of pyrazinamide in plasma and BALF were simultaneously analyzed by a non-linear mixed effects method with S-ADAPT software (v 1.52) using MC-PEM (Monte-Carlo Parametric Expectation Maximization) estimation algorithm with S-ADAPT TRAN translator [27]. Pyrazinamide PK in plasma was tested to be either mono, bi or tri compartmental. The volume of ELF compartment was fixed to a physiological volume (V_{ELF})

estimated at $30 \mu\text{L}\cdot\text{kg}^{-1}$ [28]. PK in ELF was tested to be mono-compartmental (ELF compartment), bi-compartmental (ELF + peripheral compartment) and with a depot compartment. The systemic bioavailability (F_{IT}) after intratracheal administration was estimated. The residual variability was estimated with a combined additive plus proportional error model in plasma and in ELF. Plasma concentrations below the limit of quantification were handled by Beal M3 method [29]. Likelihood ratio tests were used to compare models with a p value of 0.01 required for statistical significance. Typical values and inter-individual variability of PK parameters are reported along with the precisions of the estimates expressed as relative standard errors (RSE). Secondary PK parameters were calculated from Monte-Carlo simulations, maximal concentrations in plasma and corresponding time (C_{max} and t_{max}) were estimated directly from predicted profiles, areas under the curves (AUC) were numerically integrated, plasma half-lives were numerically estimated during terminal phase as $(dC/dt)/C$ where C is the plasma concentration, mean residence time in plasma (MRT) was numerically estimated as $AUMC/AUC$, where AUMC is the area under the first moment curve, the mean absorption time was calculated as $MRT_{\text{intratracheal}} - MRT_{\text{iv}}$, the therapeutic availability (TA) was calculated as:

$$TA = \frac{\left(\frac{AUC_{ELF}}{Dose_{\text{intratracheal}}}\right)_{\text{intratracheal}}}{\left(\frac{AUC_{ELF}}{Dose_{\text{iv}}}\right)_{\text{iv}}} \text{ and the drug targeting index (DTI) as}$$

$$DTI = \frac{\left(\frac{AUC_{ELF}}{AUC_{\text{plasma}}}\right)_{\text{intratracheal}}}{\left(\frac{AUC_{ELF}}{AUC_{\text{plasma}}}\right)_{\text{iv}}}.$$

2.7. Statistical analysis

An unpaired two-tailed *t*-test was used to test the differences between the means of two groups. A one-way ANOVA was used to test for differences between multiple groups. A two-way

ANOVA is an appropriate analysis method for a study with a quantitative outcome and two (or more) categorical explanatory variables. *P*-values <0.05 were considered as statistically significant. Correlation analysis used is the correlation coefficient (*r*) which measures the strength of a linear relation between two variables, not the agreement between them. Values between 0.7 and 1.0 (-0.7 and -1.0) indicate a strong positive (negative) linear relationship via a firm linear rule.

3. Results and Discussion

3.1. PZA-loaded LPPs preparation and characterization

In a previous study, PZA-loaded LPPs made of leucine, hyaluronic acid (HA) and dipalmitoylphosphatidylcholine (DPPC) were prepared with good yields by spray-drying using ammonium bicarbonate as a porogen [23]. Whereas spray-drying pure PZA led to agglomerated crystals (not shown) with a tap density of $0.85 \pm 0.01 \text{ g/cm}^3$, the addition of leucine and ammonium bicarbonate favored the formation of spherical particles with many pores (Fig. 1a), characterized by a reduced tap density of $0.25 \pm 0.04 \text{ g/cm}^3$ (unpaired *t*-test, *P* < 0.05). However, these particles were not stable and recrystallized over time. The addition of HA in combination with DPPC was necessary to limit the nucleation and growth of PZA crystals and yield stable partially crystalline spherical particles (Fig. 1b). The optimized formulation was obtained by spray-drying 0.9 g/L PZA, 0.6 g/L leucine, 0.2 g/L HA and 0.3 g/L DPPC and 2 g/L AB in a mixture of ethanol–water (70/30, v/v), according to conditions detailed in Table 1. The optimized powder possesses a median size of $5.8 \pm 0.1 \text{ }\mu\text{m}$ and a tap density around $0.09 \pm 0.01 \text{ g/cm}^3$. The estimated aerodynamic diameter is around $1.75 \text{ }\mu\text{m}$ and the powder is stable for

more than 4 weeks of storage. Finally, in the optimized formulation, PZA was partially crystalline as the γ polymorph, as confirmed by DSC and X-ray diffraction experiments (Fig. 2)[23].

3.2. *In-vitro* deposition

Airborne particle deposition in the human respiratory tract is highly dependent of particle aerodynamic diameter distribution [30, 31]. This distribution can be measured *in vitro* by using impactors as advised by Pharmacopoeia [24]. Impaction results are presented in Figure 3 as percent of initial dose deposited on each stage. Table 2 displays the results obtained after impaction with the optimized powder for EF, FPF, AF, MMAD and GSD. The emitted fraction is high around $99 \pm 3\%$. In spite of high emitted fraction, the FPF and AF values of optimized formulation were only about $30 \pm 3\%$ and $20 \pm 2\%$, respectively. The powder has a resulting MMAD of $5.1 \pm 0.3 \mu\text{m}$, higher than the theoretical one (MMAD_t) which was $1.75 \mu\text{m}$ [23]. Indeed, impaction results show that most of the formulation deposits in the induction port of the MSLI (Figure 3). The discrepancy between the theoretical and the experimental MMAD is frequently observed in the literature [32-34]. Previous study suggest it may be a result from the aggregation of particles during aerosolization [35]. Differences also arise from calculations: the theoretical MMAD is derived from the geometric diameter determined by laser diffraction and the tap density, while the experimental MMAD is obtained from impaction as detailed above [36]. For impaction, moisture may play a role since the MSLI contains liquid, therefore potentially inducing particle aggregation.

Observing SEM images, we noticed the coexistence of two populations of particles: large particles onto which small ones seem to be adsorbed (Figure 1b). We suspected that the composition of these two populations were not identical. We have therefore labeled the optimized formulation using a lipidic fluorescent label, Liss-Rhod-PE, which physico-chemical properties are very different from those of PZA. Impaction was then repeated following the label instead of PZA. One can notice that the two formulations do not deposit similarly, with the labeled formulation depositing deeper in the impactor. Although the EF is similar, FPF, AF and $MMAD_{aer}$ differ a lot (Table 2). These findings reflect the heterogeneous distribution of components in the particles after spray-drying. PZA and lipids do not distribute homogeneously in the powder therefore do not deposit in a similar manner.

Many previous studies report that segregation of components in multi-component mixtures could occur during the drying process [37-40]. The segregation was explained as follows. An initial layer of saturated material forms at the outside of the multi-component droplet, as evaporation proceeds, this layer thickens: the solvent moves towards the surface of the droplet, while the solutes move to the center. Solute movement towards the center of the droplet is governed by their diffusion coefficient, whereas the drying time is set by the solvent used and the gradient of temperature in the spray-dryer. The balance between these two characteristic times is summarized by the Peclet number, defined by the ratio of the mixing time of the chemicals in the droplet over the drying time of the droplet [41, 42]. This parameter however does not take into account the difference of solubility of solutes: a less soluble solute may precipitate at the interface before the other. The surface activity of solutes should also be taken into account. Since in our particular case, the spray-dryer operates at high temperature

($T_{\text{inlet}}=160\text{ }^{\circ}\text{C}$) with a mixture of ethanol-water and a large number of solutes, it is difficult to predict which of them would precipitate first at the interface.

What is known is the following. DPPC, a surfactant, is likely to position at the air - liquid surface of the droplet and to form quickly an initial layer on the surface of droplets during the spray-drying process [34, 43]. HA, a polymer of high molecular weight might not have enough time to diffuse towards the center of droplets during spray-drying. As a result, it could be trapped at the drying front leading to the earlier formation of a hollow shell [44]. Leucine is a rather hydrophobic amino acid with surface activity, driving it at the droplet surface [45, 46]. PZA is very water soluble therefore the inner part of the droplet is probably richer in PZA. Finally, since the droplet temperature is greater than 50°C , as AB sublimates it might lead to explosions and satellite droplets probably richer are PZA. However, given the complexity of the system, this remains a hypothesis and further experiments should be carried on to fully investigate the system.

To overcome heterogeneous distribution of components in the particles, while keeping solution composition constant, the spray-drying parameters were modified to decrease the drying speed: the T_{inlet} was decreased, the drying gas flow rate was reduced, the feed-flow rate was modulated and the spraying-gas flow rate was reduced as described in Table 3.

As these parameters were varied, resulting powders were characterized for their geometric diameter and aerodynamic properties (MSLI impaction). Table 4 presents the resulting T_{outlet} , D_{50} , yield, drug content, FPF, AF, MMAD_{aer} and GSD of the different samples. Results show that there are significant differences. The yield increases from 37.1% to 47.3% (unpaired t -test, $P <$

0.05), the drug content increases from 11.7% to 34.9% (unpaired t -test, $P < 0.05$), the FPF increases from 30.2% to 40.1% (unpaired t -test, $P < 0.05$), the AF increases from 19.9% to 29.6% (unpaired t -test, $P < 0.05$) and $MMAD_{aer}$ decreases from 5.1 μm to 4.1 μm (unpaired t -test, $P < 0.05$).

Correlation analysis was performed between the spray-drying parameters and the dry powders properties. This analysis shows that: i) The drying gas flow rate has a strong influences on FPF and $MMAD_{aer}$ with a negative correlation for FPF ($r = -0.80$) and with a positive correlation for $MMAD_{aer}$ ($r = 0.81$); ii) T_{outlet} influences yield, drug content and $MMAD_{aer}$ with a negative correlation for yield ($r = -0.84$) and drug content ($r = -0.97$) and with a positive correlation for $MMAD_{aer}$ ($r = 0.77$); iii) the yield increase also leads to an increase of drug content ($r = 0.86$) and the FPF increase leads to a decrease of $MMAD_{aer}$ ($r = -0.94$). In summary, reducing the drying speed will help increasing the yield, the drug content and FPF while reducing the $MMAD_{aer}$. Indeed, reducing the drying speed might minimize droplet explosions and therefore heterogeneity of the particle population composition [42]. Sample 7 conditions were finally chosen for subsequent *in vivo* experiments, since this sample exhibits suitable aerodynamic properties for dry powders delivery to the alveoli. Comparing the results in MSLI evaluation reveals that there was slightly significant difference in the deposition on each stage of sample 7 and its fluorescently-labeled counterpart (ANOVA, $P = 0.042 < 0.05$). Sample 7 composition is the following: 0.9 g/L PZA, 0.6 g/L leucine, 0.2 g/L HA and 0.3 g/L DPPC and 2 g/L AB in a mixture of ethanol–water (70/30, v/v), using the following spray-drying conditions: T_{inlet} of 140°C, a feed flow rate of 19 mL/min, a spraying gas flow rate of 473 L/h and a drying gas flow rate of 32 m³/h. The powder stability upon 4 week storage was confirmed by DSC and XRD.

3.3. *In-vivo* evaluation

The pulmonary pharmacokinetics of LPP-PZA powder after adjusting the spray-drying conditions was evaluated following administration of PZA powder corresponding to 6 mg/kg PZA as a single dose via intratracheal insufflation to rats. The amount of powder actually pushed into the lungs was 70 ± 12 % of the amount placed in the insufflator, as determined by weighing, corresponding to an administered dose by intratracheal administration of 4.22 ± 0.73 mg.kg⁻¹ of PZA. This pulmonary administration was compared to a control intravenous administration of 5.82 mg.kg⁻¹ of PZA to calculate the absolute bioavailability of our formulation. After administration, either by IV or by intratracheal administration, rats did not present apparent signs of discomfort. Mean PZA plasma concentration versus time curves are presented in Figure 4a.

From PZA concentrations in the BALF, we determined the actual PZA concentrations in the epithelial lining fluid according to dilution due to lavage. First the actual PZA concentration in the lung lining fluid was determined based on the concentration of urea in the BALF used as an endogenous marker [47] to determine the dilution factor for each animal independently (supporting information). Mean dilution factors varied in the 30-300 range leading to an unexpected result with a peak of PZA concentration at 30 min for the intratracheally administered rats (not shown). This increase of PZA concentration from 15 min to 30 min was unexpected as local concentration should decrease with time as the drug passes to the blood stream. We believe that the colorimetric method used for determination of urea concentration might not be precise enough or might suffer from interferences with PZA.

Therefore we choose to calculate the dilution factor according to the theoretical volume of epithelial lining fluid reported in the literature ($30 \mu\text{L}\cdot\text{kg}^{-1}$) and to the volume of PBS used for lavage (24mL) [28]. The resulting dilution factor for a rat of 275 g was 2910. Although this method does not take into account the dilution factor which is expected to vary for each individual rat it appears more suitable considering our experimental settings. However, considering the assumptions made to calculate the dilution factor, concentrations estimated in ELF should only be considered as relative, for comparison between the different routes of administration. PZA concentrations in the epithelial lining fluid calculated from this method are reported in Figure 4b.

In the alveolar cell pellet, PZA could only be quantified at 15 and 30 min due to the dilution of the cell pellet and the limit of quantification ($0.007 \mu\text{g}/\text{mL}$, here since we recover 2mL the limit of quantification (LOQ) is $0.014 \mu\text{g}$). There was a slight significant difference between both administration routes (Table 7) (ANOVA, $P = 0.045$) but overall amounts retrieved in alveolar cell pellets were about 1000-fold lower than those retrieved in ELF. LPPs dissolve too fast to be phagocytosed. The low concentration found in the alveolar cell pellet probably arises from PZA diffusion from the lung lining fluid.

The final model used to analyse the data in plasma and epithelial lining fluid is presented in Figure 5. The systemic part of the model was bicompartamental, characterized by a central compartment (V_c), an elimination clearance (CL) and a peripheral compartment (V_{p1}) connected to central compartment by an equilibrium distribution clearance (CL_{d1}). In the lungs, the dose was deposited in a depot compartment connected to the ELF compartment by a first order constant k_{bal} , the ELF part of the model was better fitted by two-compartments, with a

peripheral compartment (V_{p2}) connected to the central ELF compartment by two distribution clearances CL_{in} and CL_{out} , distribution between ELF and central compartment was characterized by a distribution clearance (CL_{d2}). ELF concentration was calculated as the concentration in both ELF and peripheral ELF compartments. It is of note that this two-compartment description of the ELF pharmacokinetics was necessary to fit the observed data and to make predictions but it should not be interpreted physiologically.

Data fitting was satisfactory in plasma, observed pyrazinamide concentrations scattered around typical predictions and approximately 90% of them were included in the corresponding prediction interval (Figure 6). In ELF there was one bias 6h after intratracheal administration, however it is of note that 24h after intratracheal insufflation 2 concentrations out of 6 were above the limit of quantification (15 $\mu\text{g}/\text{mL}$), i.e. above concentrations measured 6 hours post-administration. This phenomenon was described in the model by a large inter-individual variability of the PK parameters and a large residual error in the lung; the concentrations observed in ELF were inside the 90% confidence interval of predictions. It is of note that on Figure 6 concentrations measured below the limit of quantification were depicted at the LOQ value (0.01 $\mu\text{g}/\text{mL}$ in plasma and 15 $\mu\text{g}/\text{mL}$ in ELF), i.e. 4 concentrations in ELF 24h after iv administration, 4 concentrations in ELF 24h after intratracheal administration and 3 concentrations in plasma 24h after intratracheal administration. PK parameters estimated from the final model are presented in Table 6 whereas secondary parameters are presented in Table 7.

After iv administration PZA rapidly equilibrate between plasma and lung compartments with a maximal concentration in ELF predicted to occur 15 min after systemic administration.

Noticeably after iv administration PZA concentrations in ELF were much higher than in plasma (more than 100-fold, Figure 4). This might be partly due to the necessity to estimate the dilution factor in BAL and to the arbitrary choice to fix it from theoretical volumes at 2910. This value might be overevaluated, however even when using urea as endogenous marker for dilution ELF concentrations were about 10-fold higher than plasma concentrations after iv administration (not shown). This means either that there is an active transport of PZA from systemic to lung compartment either that PZA has a high affinity (or is sequestered) for some component of the lung. Actually PZA has been found to be the substrate of some ATP-dependent transport system and to penetrate into alveolar macrophages [48, 49]. However PZA amounts retrieved in alveolar cell pellets were low and the lysis of cells when practicing bronchoalveolar lavage could hardly explain such high concentrations.

After intratracheal administration, PZA crossed the lung epithelial barrier rapidly, with a peak in plasma on average 11 min after insufflation and a mean absorption time (MAT) of 0.87 ± 0.35 h, and in a relatively large extent ($F_{IT}=65.8\%$, $CV\%=14\%$). Mean residence time in plasma (MRT) was estimated to be longer after intratracheal administration than after iv administration of pyrazinamide because of the time necessary to reach ELF from the depot compartment in the former case ($k_{bal}=1.26 \text{ h}^{-1}$). This might be an advantage of intratracheal administration compared to iv administration.

Altogether, plasma, BALF and cell pellet results suggest that once PZA-LPPs are deposited in the lungs PZA is released quickly from excipients and achieves rapid distribution between plasma and lungs. This ability might arise from the mostly amorphous state of PZA in the powder but also because surface-active compounds are present in the formulation that might favor PZA

solubilization. The interest of administering the present formulation of PZA-LPPs intratracheally rather than intravenously remains moderate: (a) PZA concentrations were only 28% higher in ELF after intratracheal administration than after *iv* administration (therapeutic availability (TA)=1.28) and (b) the ratio of ELF concentrations over plasma concentrations was only 2-fold greater after intratracheal administration than after *iv* (drug targeting index (DTI)=1.97). However, these improvements might be beneficial to tuberculosis treatment and are worth investigating in infected animals.

4. Conclusion

We have optimized a formulation of pyrazinamide as large porous particles for direct lung delivery by adjusting spray drying parameters to yield homogeneous deposition of particles in the deep lungs. The *in vivo* pharmacokinetic evaluation of PZA-LPPs in rats reveals that intratracheal insufflation of PZA-LPPs lead to a rapid absorption of PZA in plasma with an absolute bioavailability of 66%, proving that PZA-LPPs dissolve fast upon deposition and that PZA crosses efficiently the lung barrier to reach the systemic circulation. PZA concentrations were 1.28-fold higher in ELF after intratracheal administration than after *iv* administration and the ratio of ELF concentrations over plasma concentrations was 2-fold greater after intratracheal administration than after *iv*. Although these improvements are moderate, lung delivery of PZA appears an interesting avenue to explore in an infected animal model to evaluate its efficacy against *Mycobacterium tuberculosis*.

Acknowledgments:

D. D. Pham fellowship is supported by Project 322, Ministry of Education and Training, VietNam. Authors thank N. Guiblin and N.E. Ghermani (SPMS, Ecole Centrale Paris) for help with X-Ray Diffraction, and V. Domergue-Dupont, A. N'Guessan and L. Aragão-Santiago for support with animal experiments. Institut Galien Paris-Sud is a member of the Laboratory of Excellence LERMIT supported by a grant from ANR (ANR-10-LABX-33).

References

- [1] R.G. Ducati, A. Ruffino-Netto, L.A. Basso, D.S. Santos, The resumption of consumption : a review on tuberculosis, *Memórias do Instituto Oswaldo Cruz*, 101 (2006) 697-714.
- [2] J.D. Grodon, Antituberculous therapy, in: L.I. Lutwick (Ed.) *Tuberculosis. A clinical handbook*, Chapman & Hall, New York, 1995, pp. 295-316.
- [3] E. Mutschler, H. Derendorf, *Drug actions : basic principles and therapeutic aspects*, Medpharm ; CRC press, Stuttgart; Boca Raton (Fla.); Ann Arbor; London [etc.], 1995.
- [4] WHO, *Global tuberculosis report 2013*, in, Geneva, Switzerland, 2013.
- [5] P. Muttill, C. Wang, A. Hickey, *Inhaled Drug Delivery for Tuberculosis Therapy*, *Pharmaceutical Research*, 26 (2009) 2401-2416.
- [6] L.V. Sacks, S. Pendle, D. Orlovic, M. Andre, M. Popara, G. Moore, L. Thonell, S. Hurwitz, *Adjunctive Salvage Therapy with Inhaled Aminoglycosides for Patients with Persistent Smear-Positive Pulmonary Tuberculosis*, *Clinical Infectious Diseases*, 32 (2001) 44-49.
- [7] D.A. Mitchison, *The action of antituberculosis drugs in short-course chemotherapy*, *Tubercle*, 66 (1985) 219-225.
- [8] Y. Zhang, D. Mitchison, *The curious characteristics of pyrazinamide: a review*, *The International Journal of Tuberculosis and Lung Disease*, 7 (2003) 6-21.
- [9] L. Heifets, P. Lindholm-Levy, *Pyrazinamide Sterilizing Activity In Vitro against Semidormant Mycobacterium tuberculosis Bacterial Populations*, *American Journal of Respiratory and Critical Care Medicine*, 145 (1992) 1223-1225.
- [10] N. Tsapis, D. Bennett, K. O'Driscoll, K. Shea, M.M. Lipp, K. Fu, R.W. Clarke, D. Deaver, D. Yamins, J. Wright, C.A. Peloquin, D.A. Weitz, D.A. Edwards, *Direct lung delivery of para-aminosalicylic acid by aerosol particles*, *Tuberculosis (Edinb)*, 83 (2003) 379-385.
- [11] G.C. Wood, J.M. Swanson, *Aerosolised Antibacterials for the Prevention and Treatment of Hospital-Acquired Pneumonia*, *Drugs*, 67 (2007) 903-914.
- [12] R. Pandey, A. Zahoor, S. Sharma, G.K. Khuller, *Nanoparticle encapsulated antitubercular drugs as a potential oral drug delivery system against murine tuberculosis*, *Tuberculosis*, 83 (2003) 373-378.
- [13] G. Chimote, R. Banerjee, *In vitro evaluation of inhalable isoniazid-loaded surfactant liposomes as an adjunct therapy in pulmonary tuberculosis*, *J Biomed Mater Res B Appl Biomater*, 94 (2010) 1-10.
- [14] P. Deol, G.K. Khuller, K. Joshi, *Therapeutic efficacies of isoniazid and rifampin encapsulated in lung-specific stealth liposomes against Mycobacterium tuberculosis infection induced in mice*, *Antimicrob Agents Chemother*, 41 (1997) 1211-1214.
- [15] P. Muttill, J. Kaur, K. Kumar, A.B. Yadav, R. Sharma, A. Misra, *Inhalable microparticles containing large payload of anti-tuberculosis drugs*, *Eur J Pharm Sci*, 32 (2007) 140-150.

- [16] S. Suarez, P. O'Hara, M. Kazantseva, C.E. Newcomer, R. Hopfer, D.N. McMurray, A.J. Hickey, Respirable PLGA microspheres containing rifampicin for the treatment of tuberculosis: screening in an infectious disease model, *Pharm Res*, 18 (2001) 1315-1319.
- [17] L. Garcia-Contreras, J. Fiegel, M.J. Telko, K. Elbert, A. Hawi, M. Thomas, J. VerBerkmoes, W.A. Germishuizen, P.B. Fourie, A.J. Hickey, D. Edwards, Inhaled large porous particles of capreomycin for treatment of tuberculosis in a guinea pig model, *Antimicrob Agents Chemother*, 51 (2007) 2830-2836.
- [18] D. Pham, E. Fattal, N. Tsapis, Pulmonary drug delivery systems for tuberculosis treatment, *Int J Pharm*, 478 (2014) 517-529.
- [19] D.A. Edwards, C. Dunbar, Bioengineering of Therapeutic Aerosols, *Annual Review of Biomedical Engineering*, 4 (2002) 93-107.
- [20] D.A. Edwards, J. Hanes, G. Caponetti, J. Hrkach, A. Ben-Jebria, M.L. Eskew, J. Mintzes, D. Deaver, N. Lotan, R. Langer, Large porous particles for pulmonary drug delivery, *Science*, 276 (1997) 1868-1871.
- [21] C.A. Dunbar, A.J. Hickey, P. Holzner, Dispersion and Characterization of Pharmaceutical Dry Powder Aerosols., *Kona*, 16 (1998) 7-45.
- [22] D.A. Edwards, Delivery of biological agents by aerosols, *AIChE Journal*, 48 (2002) 2-6.
- [23] D.D. Pham, E. Fattal, N. Ghermani, N. Guiblin, N. Tsapis, Formulation of pyrazinamide-loaded large porous particles for the pulmonary route: avoiding crystal growth using excipients, *Int J Pharm*, 454 (2013) 668-677.
- [24] Preparations for inhalation: aerodynamic assessment of fine particles - Fine particle dose and particle size distribution, in: *European Pharmacopoeia (Ph. Eur.), Addendum, Strasbourg, 2013*, pp. 309-320.
- [25] J.L. Mauderly, Bronchopulmonary lavage of small laboratory animals, *Lab Anim Sci*, 27 (1977) 255-261.
- [26] J.E. Conte, Jr., E. Lin, E. Zurlinden, High-performance liquid chromatographic determination of pyrazinamide in human plasma, bronchoalveolar lavage fluid, and alveolar cells, *J Chromatogr Sci*, 38 (2000) 33-37.
- [27] J.B. Bulitta, A. Bingolbali, B.S. Shin, C.B. Landersdorfer, Development of a new pre- and post-processing tool (SADAPT-TRAN) for nonlinear mixed-effects modeling in S-ADAPT, *Aaps J*, 13 (2011) 201-211.
- [28] A.V. Gontijo, J. Brillault, N. Gregoire, I. Lamarche, P. Gobin, W. Couet, S. Marchand, Biopharmaceutical characterization of nebulized antimicrobial agents in rats: 1. Ciprofloxacin, moxifloxacin, and grepafloxacin, *Antimicrob Agents Chemother*, 58 (2014) 3942-3949.
- [29] S.L. Beal, Ways to fit a PK model with some data below the quantification limit, *J Pharmacokinet Pharmacodyn*, 28 (2001) 481-504.
- [30] M. Dolovich, Measurement of particle size characteristics of metered dose inhaler (MDI) aerosols, *J Aerosol Med*, 4 (1991) 251-263.
- [31] C. Papastefanou, Aerosol sampling and measurement techniques, in: *Radioactive Aerosols*, Elsevier, Greece, 2008, pp. 113-159.
- [32] Aliasgar J. Kundawala, Vishnu A. Patel, Harsha V. Patel, D. Choudhary., Influence of Formulation Components on Aerosolization Properties of Isoniazid Loaded Chitosan Microspheres., *International Journal of Pharmaceutical Sciences and Drug Research*, 3 (2011) 297-302.
- [33] C. Bosquillon, C. Lombry, V. Pr eat, R. Vanbever, Influence of formulation excipients and physical characteristics of inhalation dry powders on their aerosolization performance, *Journal of Controlled Release*, 70 (2001) 329-339.
- [34] C. Bosquillon, P.G. Rouxhet, F. Ahimou, D. Simon, C. Culot, V. Pr eat, R. Vanbever, Aerosolization properties, surface composition and physical state of spray-dried protein powders, *Journal of Controlled Release*, 99 (2004) 357-367.

- [35] C. Bosquillon, V. Pr eat, R. Vanbever, Pulmonary delivery of growth hormone using dry powders and visualization of its local fate in rats, *Journal of Controlled Release*, 96 (2004) 233-244.
- [36] G. Pilcer, F. Vanderbist, K. Amighi, Correlations between cascade impactor analysis and laser diffraction techniques for the determination of the particle size of aerosolised powder formulations, *International Journal of Pharmaceutics*, 358 (2008) 75-81.
- [37] E.L. Cussler, *Diffusion: Mass Transfer in Fluid Systems*, 2nd ed., Cambridge University Press 1997.
- [38] B. Adhikari, T. Howes, A. Shrestha, B.R. Bhandari, Effect of surface tension and viscosity on the surface stickiness of carbohydrate and protein solutions, *Journal of Food Engineering*, 79 (2007) 1136-1143.
- [39] M. Cano-Chauca, P.C. Stringheta, A.M. Ramos, J. Cal-Vidal, Effect of the carriers on the microstructure of mango powder obtained by spray drying and its functional characterization, *Innovative Food Science & Emerging Technologies*, 6 (2005) 420-428.
- [40] O.R. Roustapour, M. Hosseinalipour, B. Ghobadian, An Experimental Investigation of Lime Juice Drying in a Pilot Plant Spray Dryer, *Drying Technology*, 24 (2006) 181-188.
- [41] N. Tsapis, D. Bennett, B. Jackson, D.A. Weitz, D.A. Edwards, Trojan particles: Large porous carriers of nanoparticles for drug delivery, *P Natl Acad Sci USA*, 99 (2002) 12001-12005.
- [42] G. Marty, N. Tsapis, Monitoring the buckling threshold of drying colloidal droplets using water-ethanol mixtures, *Eur Phys J E*, 27 (2008) 213-219.
- [43] A. Minne, H. Boireau, M.J. Horta, R. Vanbever, Optimization of the aerosolization properties of an inhalation dry powder based on selection of excipients, *European Journal of Pharmaceutics and Biopharmaceutics*, 70 (2008) 839-844.
- [44] C. G omez Gaete, N. Tsapis, L. Silva, C. Bourgaux, E. Fattal, Morphology, structure and supramolecular organization of hybrid 1,2-dipalmitoyl-sn-glycero-3-phosphatidylcholine-hyaluronic acid microparticles prepared by spray drying, *European Journal of Pharmaceutical Sciences*, 34 (2008) 12-21.
- [45] R. Wolfenden, L. Andersson, P.M. Cullis, C.C.B. Southgate, Affinities of amino acid side chains for solvent water, *Biochemistry*, 20 (1981) 849-855.
- [46] J. Gliński, G. Chavepeyer, J.-K. Platten, Surface properties of aqueous solutions of l-leucine, *Biophysical Chemistry*, 84 (2000) 99-103.
- [47] E. Kipnis, Using urea as an endogenous marker of bronchoalveolar lavage dilution, *Crit Care Med*, 33 (2005) 2153; author reply 2153-2154.
- [48] S. Kiem, J.J. Schentag, Interpretation of antibiotic concentration ratios measured in epithelial lining fluid, *Antimicrob Agents Chemother*, 52 (2008) 24-36.
- [49] C. Raynaud, M.A. Laneelle, R.H. Senaratne, P. Draper, G. Laneelle, M. Daffe, Mechanisms of pyrazinamide resistance in mycobacteria: importance of lack of uptake in addition to lack of pyrazinamidase activity, *Microbiology (Reading, England)*, 145 (Pt 6) (1999) 1359-1367.

Table 1: Operational conditions used for spray drying the initial optimized formulation

Spray drying parameters	Operational conditions
Feed-flow rate	11 mL/min
Inlet temperature (T_{inlet})	160°C
Outlet temperature (T_{outlet})	81°C
Drying gas flow rate	38 m ³ /h
Spraying gas flow rate	498 L/h

Table 2: Aerodynamic properties of the optimized formulation and fluorescently-labeled formulation (mean \pm SD, n= 2)

	Optimized formulation (unlabeled)	Optimized formulation (fluorescently-labeled)
EF (%)	99 \pm 3	98 \pm 1.5
FPF (%)	30 \pm 3	45 \pm 3
AF (%)	20 \pm 2	36 \pm 4
MMAD (μm)	5.1 \pm 0.3	3.7 \pm 0.3
GSD	2.0 \pm 0.1	2.5 \pm 0.6

Table 3: Spray drying parameters modified to optimize the aerodynamic properties of the powder.

Sample	Spray drying Conditions				
	T _{inlet} (°C)	Drying gas	Feed Flow	Spraying gas	T _{outlet} (°C)
		flow rate (m ³ /h)	Rate (mL/min)	flow rate (L/h)	
1	160	38	11	498	81
2	140	38	11	473	69
3	120	38	10	414	63
4	120	32	10	414	56
5	120	38	10	473	62
6	140	38	19	414	63
7	140	32	19	473	53

Table 4: Powder characteristics according to the spray drying conditions (mean \pm SD, n= 2). The finally selected formulation is highlighted.

Sample	D ₅₀ (μm)	Yield (%)	Drug Content (%)	FPF (%)	AF (%)	MMAD (μm)	GSD
1	5.6 \pm 0.3	37.1 \pm 5.9	11.7 \pm 2.5	30.2 \pm 3.2	19.9 \pm 2.3	5.1 \pm 0.3	1.99 \pm 0.06
2	6.4 \pm 1.4	39.1 \pm 1.1	26.2 \pm 2.0	32.0 \pm 7.5	22.8 \pm 7.9	4.7 \pm 0.8	1.99 \pm 0.12
3	7.0 \pm 0.1	48.4 \pm 0.3	30.5 \pm 3.9	28.4 \pm 1.8	17.6 \pm 0.4	4.9 \pm 0.1	1.83 \pm 0.06
4	5.9 \pm 0.4	47.6 \pm 0.5	34.2 \pm 1.6	33.0 \pm 2.3	21.2 \pm 1.9	4.6 \pm 0.1	1.88 \pm 0.02
5	4.7 \pm 0.7	42 \pm 0.0	27.2 \pm 0.6	28.7 \pm 1.6	19.0 \pm 1.2	4.9 \pm 0.1	1.97 \pm 0.02
6	6.5 \pm 0.1	42.6 \pm 0.0	27.7 \pm 2.1	30.7 \pm 0.5	19.9 \pm 0.8	4.9 \pm 0.1	1.86 \pm 0.00
7	5.3 \pm 0.1	47.3 \pm 0.8	34.9 \pm 2.2	40.1 \pm 1.0	29.6 \pm 3.1	4.1 \pm 0.2	2.16 \pm 0.16

Table 5: Amount of PZA in alveolar cell pellet versus times (mean \pm SD, n= 6).

	Time	15 min	30 min	3 h	6 h	24 h
PZA (μg)	iv	0.037 \pm 0.023	0.060 \pm 0.055	< LOQ		
	Intratracheal	0.044 \pm 0.015	0.022 \pm 0.012			

Table 6: Estimation of PK parameters after intratracheal administration and iv administration of pyrazinamide at doses 4.22 and 5.82 mg.kg⁻¹, respectively.

		Typical value (RSE%)	Interindividual variability (RSE%)
V _c	(mL.kg ⁻¹)	8.82 (54%)	34% (126%)
V _{p1}	(mL.kg ⁻¹)	326 (1%)	
V _{p2}	(μL.kg ⁻¹)	6.27 (3%)	
V _{ELF}	(μL.kg ⁻¹)	30 Fixed (-)	-
F _{IT}	(%)	65.8 (5%)	14% (46%)
CL	(L.h ⁻¹ .kg ⁻¹)	0.133 (3%)	
CLd ₁	(L.h ⁻¹ .kg ⁻¹)	0.305 (11%)	9% (111%)
CLd ₂	(L.h ⁻¹ .kg ⁻¹)	0.298 (5%)	-
CLd _{lung1}	(mL.h ⁻¹ .kg ⁻¹)	44.9 (10%)	50% (34%)
CLd _{lung2}	(mL.h ⁻¹ .kg ⁻¹)	0.0974 (2%)	-
k _{lung}	(h ⁻¹)	1.26 (17%)	41% (73%)
Matrix	Residual error		
Plasma	Additive(μg/mL)	0.037 (23%)	
	Proportional (%)	18% (13%)	
ELF	Additive(μg/L)	41 (103%)	
	Proportional (%)	-	

^a RSE, Relative Standard Error expressed as coefficient of variation.

V_c, volume of distribution in central compartment; V_{p1}, volume of distribution of peripheral compartment; V_{p2}, volume of distribution of lung peripheral compartment; V_{ELF}, volume of distribution of ELF compartment; F_{IT}, systemic bioavailability after intratracheal administration, CL, total systemic clearance; CLd₁, clearance of distribution between central and peripheral compartments; CLd₂, clearance of distribution between central and ELF compartment; CLd_{lung1}, clearance of distribution from ELF compartment towards lung peripheral compartment; CLd_{lung2}, clearance of distribution from lung peripheral compartment towards ELF compartment; k_{lung}, first order transfer rate constant from depot compartment towards ELF compartment.

Table 7: Secondary PK parameters (mean \pm SD) after iv and intratracheal administrations of pyrazinamide at doses 5.82 and 4.22 mg.kg⁻¹ respectively.

Pharmacokinetic parameters	iv administration	Intratracheal administration
C _{max} (μg/mL)	9.09 \pm 0.69	7.47 \pm 2.89
t _{max} (h)	NA	0.19 \pm 0.12
AUC (μg.h/mL)	44.0 \pm 0.0	21.2 \pm 3.0
t _{1/2} (h)	2.52 \pm 0.07	2.52 \pm 0.07
MRT (h)	2.57 \pm 0.03	3.44 \pm 0.35
MAT (h)	NA	0.87 \pm 0.35
Therapeutic Availability	NA	1.28 \pm 1.10
Drug Targeting Index	NA	1.97 \pm 1.73

C_{max}, maximal concentration in plasma ; t_{max}, time of maximal concentration in plasma ; AUC, area under the curve of plasma concentrations ; t_{1/2}, terminal half-life in plasma, MRT ; mean residence time ; MAT, mean absorption time.

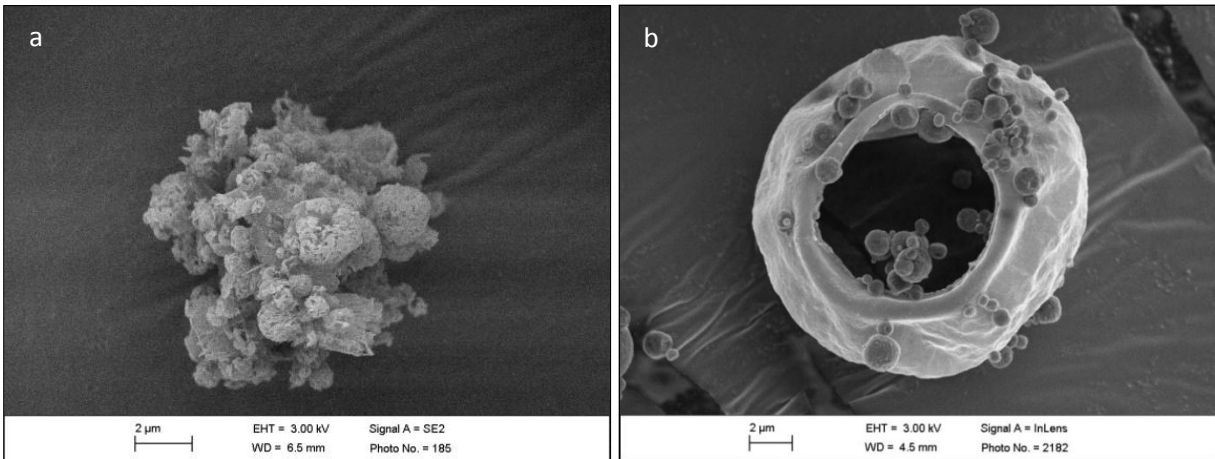


Figure 1: SEM micrographs of spray dried PZA particles containing leucine (a) or leucine added with HA and DPPC (b) where one can notice the coexistence of a large hollow particle on which small dense particles are adsorbed.

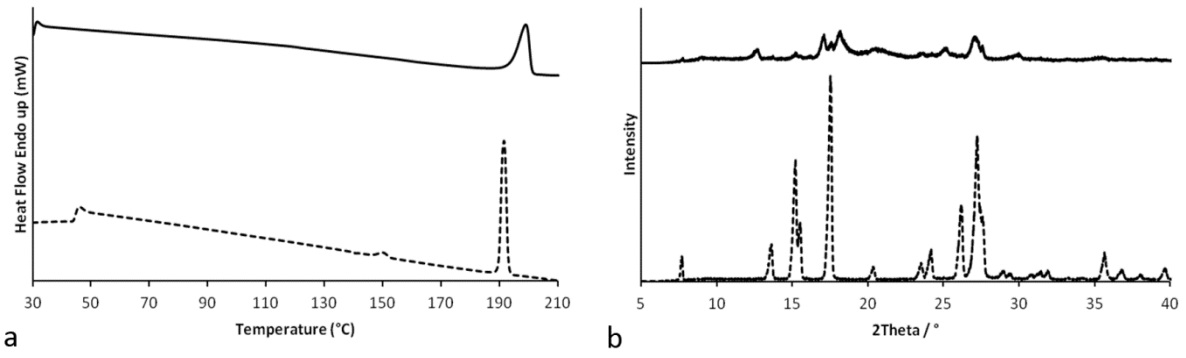


Figure 2: a: DSC thermograms of raw PZA (dotted line) and the optimized formulation (full line).

b: X-Ray diffraction patterns obtained for raw PZA (dotted line) and the optimized formulation (full line).

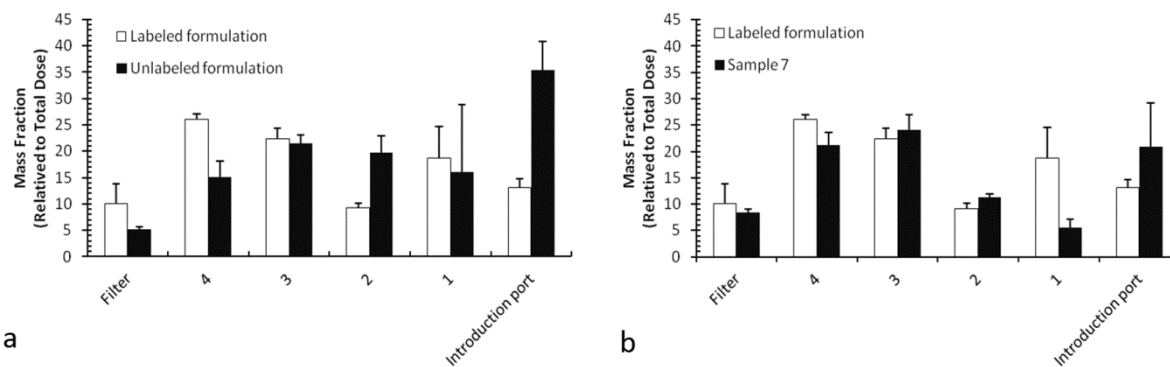


Figure 3: Comparison of impaction results obtained for the initially optimized formulation (unlabeled formulation) and its labeled counterpart (a); for sample 7 and its labeled counterpart (b).

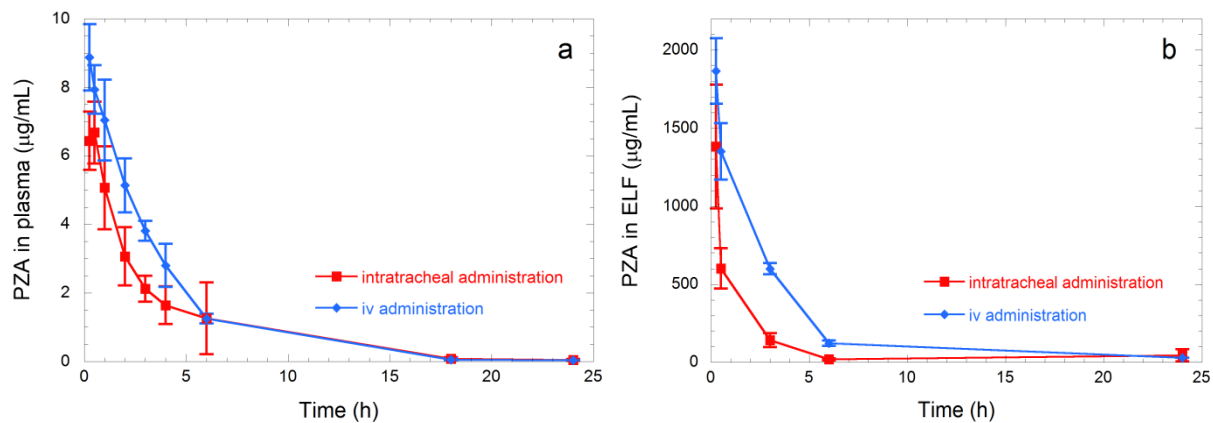


Figure 4: PZA Plasma concentration (a) and ELF concentration using a constant dilution factor for the lavage (2910) (b) as a function of time after intratracheal ($4.22 \text{ mg}\cdot\text{kg}^{-1}$) and intravenous administration ($5.82 \text{ mg}\cdot\text{kg}^{-1}$).

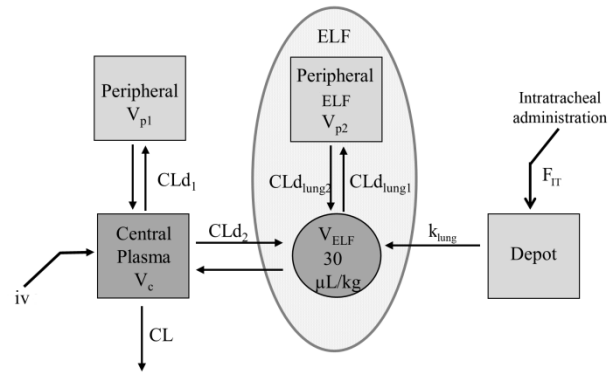


Figure 5: Structural model

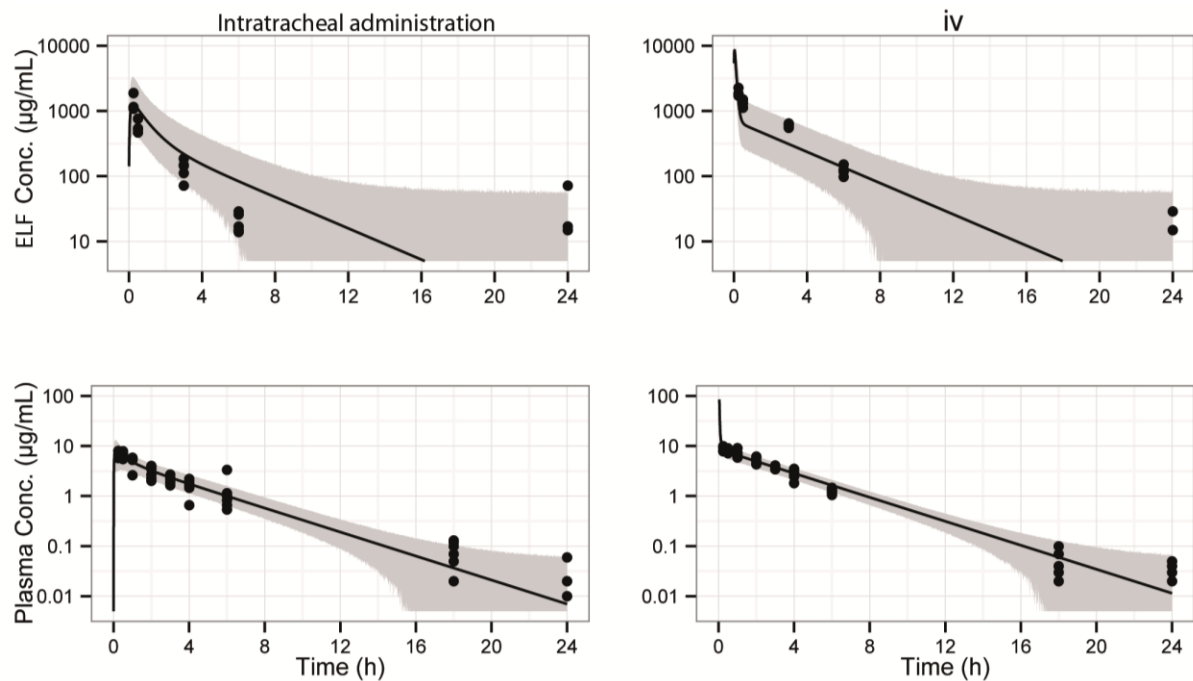


Figure 6: Individual (dots) observed pyrazinamide concentrations along with model typical (solid line) and IC90% (grey area) predictions after intratracheal (4.22 mg.kg^{-1}) and intravenous administration (5.82 mg.kg^{-1}).